SEMARAK ILMU PUBLISHING

Journal of Advanced Research in Applied Sciences and Engineering Technology

Journal homepage:
https://semarakilmu.com.my/journals/index.php/applied_sciences_eng_tech/index
ISSN: 2462-1943

Passively Q-Switched 1.5- µm Erbium-Doped All-Fibre Laser with Silver Saturable Absorber

Kawther M. Musthafa[1], Azura Hamzah[1,*], Farouk Al Ghifarry[1], Ooi Wei Ling[1], Haziq Aiman Rosol[1]

[1] Malaysia-Japan International Institute of Technology (MJIIT), Universiti Teknologi Malaysia, Jalan Sultan Yahya, 54100 Kuala Lumpur, Malaysia

ARTICLE INFO

Article history:
Received 2 June 2023
Received in revised form 25 August 2023
Accepted 31 October 2023
Available online 20 March 2024

Keywords:

Q-switch; Erbium doped fibre (EDF); All-fibre laser; Saturable absorber

ABSTRACT

This research examines the operation of a passively Q-switched erbium-doped all-fibre laser (EDFL) using a silver (Ag) based saturable absorber (SA) by comparing the output characteristics of the Q-switched laser with those of continuous wave all-fibre lasers. A study was done on how the laser's Q-factor is modified and affects the rate at which pulses are repeated, as well as their output power, width, and energy. The results showed that high-energy Q-switched pulses were successfully generated at the essential 1.5 µm wavelength within the pump power range of 83.6 mW to 171.7 mW, with repetition rates ranging from 33.46 kHz to 77.96 kHz. The EDFL generated a pulse with a width of 4.033 µs and an energy of 2.82 nJ at a pump power of 171.7 mW. The results indicate that *Ag* may potentially be a good SA for pulse production in the 1.5 µm wavelength area as well as for use in a wide range of applications.

1. Introduction

Attributable to their special qualities, such as an easy laser setup and the ability to produce picosecond and femtosecond [1] pulsed lasers, pulsed all-fibre ring cavity lasers have been patented and are now being used in a wide range of applications, including sensors [2], optical communication, digital services, spectroscopy, micromachining [3], medical systems and biomedicine [4], and material processing [5]. Resistance to disturbance, upright beam quality, and high energy conversion efficiency are some other favourable qualities. Since then, several applications have shown potential, especially with pulse durations quicker than a picosecond, such as ophthalmology [6], bio-imaging, molecular spectroscopy [7], and nonlinear microscopy [8]. Only two near-infrared (NIR) wavelengths—a high-power ultrafast laser at 1064 nm and long-distance telephony at 1550 nm—are thought to be more pertinent for the majority of these applications [9].

The primary methods for creating pulsed lasers, mode-locking, and Q-switching, can be further divided into two modulation types: passive modulation [10], which entails placing a saturable absorber (SA) inside the laser cavity, and active modulation, which involves using an active modulator to regulate the cavity loss periodically. Both procedures have respective advantages [11], though

* *Corresponding author.*
E-mail address: azurahamzah@utm.my

https://doi.org/10.37934/araset.41.2.1830

passive Q-switching proposes a simpler design without the use of gigantic optical modulators [12] with convoluted and bulky systems that frequently restrict flexibility. This evidently becomes significant when considering the expenses of production, beam quality, and energy effectiveness [13]. The conventional strategy of passive Q-switch employs SAs, a nonlinear optical material with an intensity-dependent light diffusion property, to add a spoiling to the quality factor mechanism. An ideal SA may be found by considering factors like quicker recovery time for broadband absorption, high depth modulation, high bleaching threshold, simplicity of fabrication [14], and affordability.

Two different types of SAs are used to create passive pulsed lasers. One is based on the Kerr lens and relies on nonlinear and/or birefringent processes, while the other uses linear effects. An explanation for how light interacts with SA matter is provided by the phenomenon of nonlinear optics. In particular, nonlinearity sheds light on how materials react to variations in the strength of the applied electromagnetic field [15]. As a result of the nonlinearity effect, saturable absorption is one of the intriguing optical phenomena that is rapidly emerging. Ultrashort pulsed lasers of picosecond or even femtosecond duration can be produced using saturable absorption. Although optical loss decreases as light intensity increases, SAs show intensity-dependent transmission [16]. The SA, a passive component, activates pulsed laser light using the passive switching mechanism of an all-fibre laser cavity. Due to the predicted benefits of system size and mobility, cost-effectiveness, enhanced beam quality, and superior heat intemperance of the fibre, the development of fibre lasers with extraordinary features has attracted a lot of interest [17].

There are numerous distinct kinds of SAs, including transition metal dichalcogenides (TMD) [18], carbon nanotubes (CNT), graphene, semiconductor saturable absorbers (SESAM) [19], and other 2D material groups. In addition to these, noble metal SAs have grown in popularity because of their exceptional qualities. The majority of them are appropriate for purposes in telecommunications, welding and cutting in industry, and medical procedures including surgery, tattoo removal, and skin resurfacing. Despite this, some of these materials could encounter difficulties when employed for certain purposes, particularly in medical settings like surgery. As larger spectrum SAs are desirable for specific purposes, medical surgery might pose difficulties due to the relatively restricted absorption range of metals like platinum and palladium. The range of wavelengths over which both SAs can work efficiently may be constrained by this limited absorption range [20]. Gold's use for high-power laser systems that need heat dissipation may be constrained by its generally lower melting point and lower thermal conductivity. Platinum, palladium, and gold are all regarded to be scarce elements, making them very expensive, although cost-effectiveness in applications is crucial [21].

Silver (Ag), another noble metal, is recommended as an alternate SA [22] material to get around these restrictions. Due to its large absorption spectrum, Ag may interact with a wide range of wavelengths [23]. Due to the requirement for various wavelengths or a broad spectrum in laser systems for use in industrial applications, this might be helpful [4]. Ag may be utilised for a longer period and can tolerate exposure to greater-intensity laser pulses since it has a higher melting point and damage threshold than gold. Last but not least, compared to other SAs, Ag is often the most affordable.

With an atomic number of 47, Ag is an element belonging to group 11 and the fifth period. Ag is a transition element and one of the noble metals [24], along with gold and copper. The intriguing optical characteristics of this material have attracted a lot of attention. It benefits from the broad-band saturable absorption of surface plasmon resonance (SPR), which extends into the infrared [25]. As a result, Ag is a suitable SA for pulsed-wave (PW) fibre laser operations at many wavelengths. Previous studies have looked into employing Ag as an SA to create PW fibre lasers using the Q-switching technique. In the first experiment, Guo *et al.,* used an erbium-doped cavity to create a passively Q-switched PW laser in the C-band (1530 – 1565 nm) [26].

The goal of this study is to compare the performance of fibre lasers that contain Ag-SA and those that do not, as well as to evaluate several characteristics, such as repetition rate, output power, pulse energy, and pulse width. The research's relevance lies in its potential for Ag to replace SA, stressing its high damage threshold, wide absorption spectrum, reliable output, accurate energy delivery, and cost-effective materials for particular applications [27].

2. Methodology

The SA has been fabricated using chemical reduction technique and an all-fibre laser ring cavity has been built up. This cavity was set up to emit Q-switched laser pulses utilising a fibre laser gain medium that is doped with erbium.

2.1 Fabrication and Preparation

Ag-SA was fabricated utilising a chemical reduction process. By employing a host polymer to attach the Ag particles, this technique creates high-quality SAs easily and economically [10,28]. PVA solution is odourless, colourless, and eco-friendly and it works well as a host polymer. PVA is an excellent host polymer that does not change the material's inherent Q-switched function, according to Ahmad *et al.,* [29]. Therefore, in this fabrication, PVA solution was used as the host polymer to hold the Ag particles together and create a usable SA thin film [30]. This process was broken down into three key steps: making the PVA solution, making the Ag solution, and combining the two [31]. Chemical reduction techniques were used to create the colloidal Ag nanoparticles [32]. The Ag nanoparticles were recovered by centrifugation at 6000 rpm for 30 min to separate the Ag and excess agent to make the *Ag-PVA* SA. To guarantee that all of the excess agent was removed, the colloidal Ag was centrifuged three times while being refilled with deionized water (DIH_2O) each time. The aqueous PVA solution was made by mixing 60 mL of DIH_2O with 0.5 g of PVA powder (40,000 MW, Sigma Aldrich) and heating it to 145 °C until the powder completely dissolved. After that, Ag was diluted into the PVA solution at a ratio of 1:5 (mg/mL) and ultrasonically processed for an hour before being stirred for another three hours. The *Ag-PVA* solution was then decanted into a 5 ml petri plate and allowed to dry for 3 days in the desiccator cabinet. The film was maintained in an air-tight bag after being gently peeled off to create a free-standing film-based SA. By measuring the lattice spacing and comparing it to the plane of Ag from earlier research, the crystalline nature of a single particle was further investigated [33]. The chemical reduction method's sluggish reaction rate ameliorated the reactions, whereby particle sizes were found between 50 and 100 nm [34]. The result was An Ag-PVA SA with a diameter of 30 mm. Following the application of optical indexing gel, the Ag-PVA SA was sliced into a size of around 1 mm^2 for incorporation in a Q-switched EDFL ring cavity design.

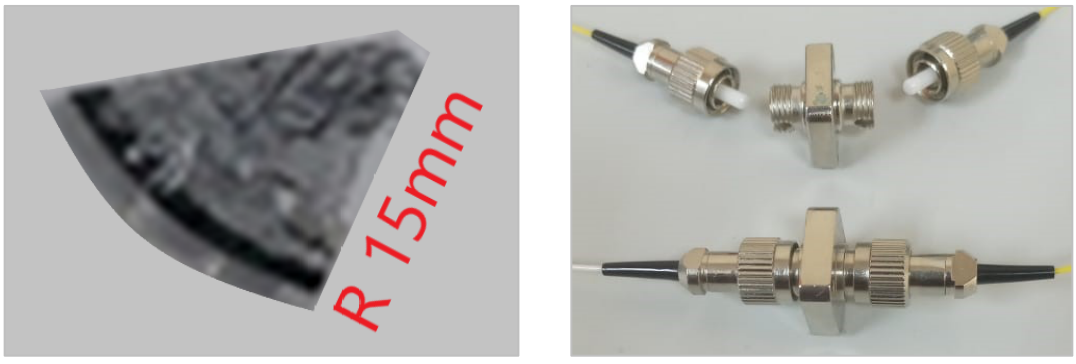

Fig. 1. Silver (Ag) based saturable absorber (a) SA thin film, (b) SA incorporated ferrule

Basic physical characterisation was carried out to determine the distribution of the Ag nanomaterial on the thin film by thickness and surface morphology before the thin film was used as an SA in the Q-switching ring cavity setup. Thus, the atomic ratios, distribution, kind, and arrangement of the fabricated Ag SA would serve as proof of its availability. Then a 980 nm LD source (Q-photonics, QFLD-405-20S)—acting as an amplifier and power booster—that pumps the laser cavity in the tabletop laser controller (GOOCH & HOUSEGO, EM595 was characterised for its output power. The input current was fed via a 980/1550 nm wavelength division multiplexer (WDM 980/1550nm), which multiplexes optical signals of different frequencies. The input pump power in the range of 0 to 350 mA was then measured using an optical power meter (OPM; Thorlabs, PM100D) to calculate the laser diode power in milliwatts (mW). The data was represented graphically with a curve-fitting equation applied. Linear rises in mW of pump power versus mA demonstrate a stable operational wavelength range with the highest steady pumping attained at 350-mA pump power. Essentially, to obtain pulse stability, the pump power range was determined to be from 40 mA to 350 mA (3.5 mW to 177.6 mW).

$$y = 0.56161x - 18.96452 \quad (1)$$

The curve fitting equation above further explains the pump characterisation of pump power after WDM: where y represents the y-axis, LD power in milliwatts, and x represents the x-axis, LD current in milliamperes. This equation illustrates the connection between the input pump power and the current supply of the LD diode.

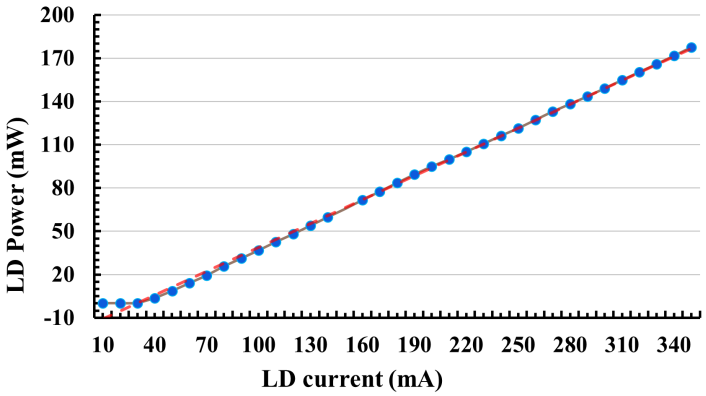

Fig. 2. Characterisation of benchtop LD pump

2.2 Q-Switched All-Fibre Ring Cavity Configuration

As shown in Figure 3, the foundation for the laser cavity was created by carefully positioning and splicing the optical and optoelectronic components to create a ring-shaped cavity of the all-fibre laser design. To begin unidirectional pumping, a 980 nm laser diode (LD) was shot via a wavelength division multiplexer (980 nm arm). The input optical pump signal at 980 nm and the feedback signal at 1550 nm were multiplexed by the WDM. The light was then focused into a 2.4 m long erbium-doped fibre (EDF) for signal amplification. The EDF (SM-ESF-7/125) has a 7-µm mode field diameter, a 125.4-µm fibre diameter, a 0.24 numerical aperture (NA), and a 20.1 dBm^{-1} absorption coefficient at 986 nm. By coupling the EDF to a polarisation-independent isolator (PI-ISO), a unidirectional light flow was ensured. In addition to preserving the LD pump, this PI-ISO is also essential in preventing light from backflowing into the LD pump. Consensual light may damage the laser diode and reflect backwards

within the cavity, producing irregular laser pulses. The optical coupler that the isolator was connected to has an 80:20 splitting ratio. A clean fibre adapter was used to join the two fibre ferrules.

An experiment was carried out by attaching the EDFL ring cavity configuration with and without the Ag-SA to an optical spectrum analyser (OSA; Yokogawa, AQ6370D) in order to determine the significance of its presence in generating the pulsed laser output. Through this study, the SNR value and wavelength shifting of these EDFL ring cavity topologies are seen. The performance characteristics of the Ag-SA-based Q-switched EDFL ring cavity arrangement were tested. A Q-switched fibre laser's performance parameters primarily pertain to the variables that influence how the Q-factor is modulated as shown in Eq. (1).

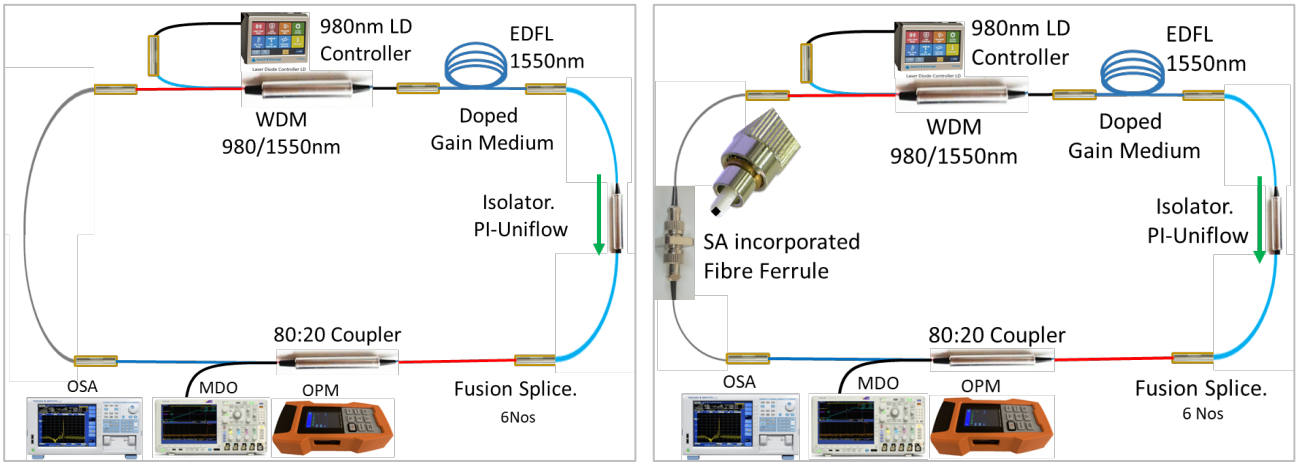

Fig. 3. EDFL all-fibre ring cavity configuration (a) CW configuration, (b) PW configuration

A cavity with a net group delay dispersion (GDD) of -0.17744ps^2 is produced by a 2.4 m long gain medium with a group velocity dispersion (GVD) of -21.6 ps^{2}km^{-1}, a 4 m long SMF equivalent with a -21.9 ps^{2}km^{-1}, and yet another 1 m with a -38.0 ps^{2}km^{-1}. Two main factors influence the Q-switched pulse width. The following mathematical equation links cavity loss with the elongation of the erbium-doped gain fibre [4].

$$\Delta_t = -\int_{\Delta_n}^{\Delta_{ni}} \frac{d\Delta_n}{\Delta_n(\Delta_{ni}/\Delta_{nt} - \Delta_n/\Delta_{ni} + \ln\Delta_n/\Delta_{ni})} \tag{2}$$

Where Δ_n denotes the population inversion density, Δ_{ni} the maximum inversion density, and Δ_{nt} the threshold inversion density. The primary factor influencing Q-switched pulse width is Δ_{nt}; a lesser Δ_{nt} will result in a narrower pulse width. Therefore, the pulse width may be reduced even further by reducing cavity loss and lengthening the gain fibre doped with erbium.

The fabricated Ag-SA thin film was split into about 1 mm^2 and positioned in between the end facets of FC/PC optical fibre ferrules for the research of various ratios of Ag-SA as a Q-switcher. The optical spectrum analyser (OSA; Yokogawa, AQ6370D) was then linked to the 5% light signal coupled out in order to examine the optical spectrum of Ag-SA. The linked signal is then connected to a mixed domain oscilloscope (MDO; TEKTRONIX, MDO3024) to analyse the pulse repetition rate f_R and pulse width Δt, the temporal characteristics of the pulse train produced.

$$U = \frac{P_{avg}}{f_R} \tag{3}$$

The following power-related characteristics were examined: the optical output power P_{avg} is measured using an optical power meter (OPM; THORLABS, PM100D), and the pulse energy U was calculated using Eq. (3). To achieve the desired condition of having comparatively high output power, high repetition rate, high pulse energy, and small pulse width, the performance characteristics were evaluated to establish the appropriate ratio.

3. Results

A 10-mA step was used to raise the pump power from 0 mA to 350 mA. 5.217 mW is the equivalent of this step according to the pump characterization that was done. When the cavity began to function, the pump was adjusted with even better resolution to determine the precise threshold point with a single decimal accuracy. This number, 36.7 mW, was discovered to be comparably low for a Q-switched cavity to begin operating in CW mode. The two factors that contributed to the CW's low pump power threshold were the enhanced splicing with zero with minimum loss and the optimised laser cavity length.

It was found that Q-switching activity employing the SA made of Ag started at a threshold pump power of 48.2 mW, but that it gave highly steady pulses starting at 83.6 mW up to the entire range of the pump, which is 171.7 mW. No pulse train was found when the Ag-fabricated SA was removed from the cavity. These findings support the fact that the Ag-fabricated thin film functions in creating Q-switching pulses.

Throughout the approximately four-week testing, the Ag film did not physically deteriorate. Because of the film's consistent performance at this highest incident intensity, its specific absorbance is likely significantly higher than the optical intensity of 171.7 mW across an SMF with a diameter of less than 7 µm. The optical frequency spectrum of the Q-switched EDFL created utilising Ag film as the SA at 171.7 mW pump power is shown in Figure 4. The Q-switched laser has a 2.4 nm spectral bandwidth, which corresponds to a centre wavelength of 1590.7 nm.

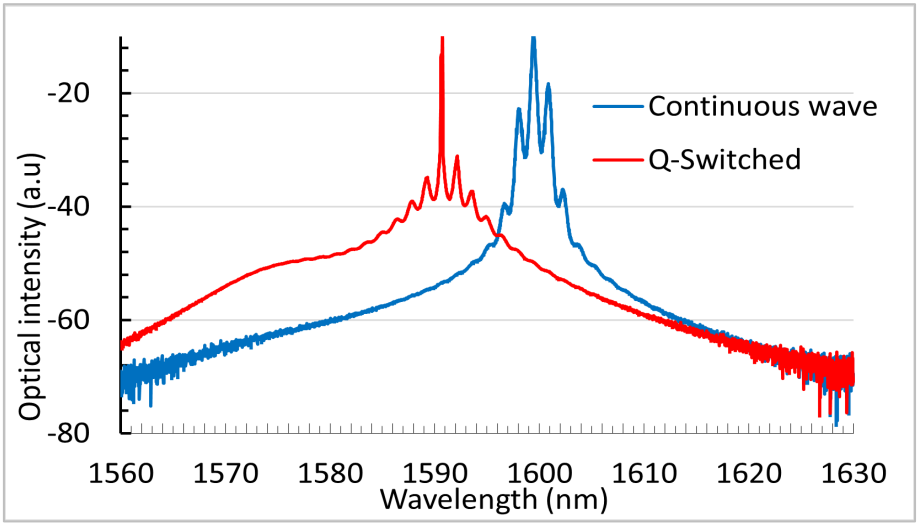

Fig. 4. Optical spectrum trace of continuous and pulsed wave laser output

The resonant frequency of PW lasers shifts to the right (right-shift) in comparison to CW because of self-phase modulation and intracavity loss that the PW spectrum experiences within the laser cavity configuration when the SA is inserted. This causes blue-shifting, an increase in operating PW frequency, or a decrease in wavelength.

Due to "self-phase modulation," a nonlinear optical phenomenon where the optical Kerr effect causes all cavity fibre components, including EDFL, to change their refractive index in response to a brief pulse, causing a phase shift in the pulse and changing its frequency spectrum, the operating bandwidth broadens from less than 1 nm to more than 2 nm.

It can be seen that the average output power (P_{av}) scales linearly with the input power since the output power for the continuous wave (without SA) increases in direct proportion to the laser pump input. The continuous wave output power increases from 0.266 mW to 9.27 mW when the laser pump input is raised from 36.7 mW to 149.1 mW. In contrast, as the laser pump increases, as depicted in Figure 5, the output power of the Q-switched PW also begins to rise linearly from 0.63 mW to 3.20 mW, though with a lower gradient than the CW output due to insertion loss (linear absorption). It is noted that the insertion loss exhibits a proposed behaviour for the intensity. The peak pulse power (P_{pk}) during the duty cycle will be much more than that of the CW.

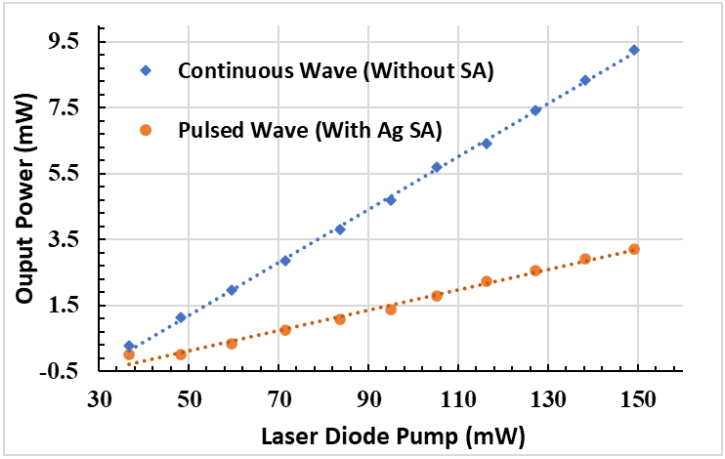

Fig. 5. Output power of continuous and pulsed wave laser output with LD pump

As the laser pump input rises, the SA reaches a certain point where it begins to saturate and allows a greater proportion of energy to be supplied. Due to its greater output power levels, the PW is suitable for applications that call for strong and short laser pulses.

In a passive Q-switched laser, a cavity-mounted SA, in this instance, the Ag-SA—that normally functions on saturable absorption—controls the laser output. The SA effectively absorbs the incoming light when the laser input power is low, preventing it from passing through the laser cavity. The outcome is a modest laser output power and a generally stable (low fluctuating) power supply. The decreased average output power stability figures for lower laser input powers such as 83.6 mW and 95 mW demonstrate this.

The bigger average output power figures for higher laser input powers (such as 160.4 mW and 171.7 mW) indicate that in a passively Q-switched laser utilising Ag SA, the relationship between laser input power and the average steady output power is often nonlinear. As the laser input power passes a specific threshold and the SA becomes highly saturated, the power stability begins to degrade. Beyond this, the output power variations are more noticeable, leading to increased average output power instability. It is crucial to remember that the properties of the SA material and the laser cavity design can affect the precise connection between laser input power and power stability.

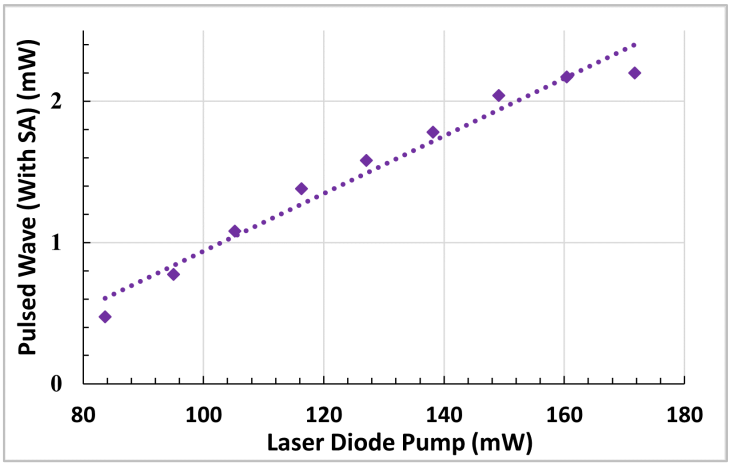

Fig. 6. Stability of output power with LD pump

By enabling the laser cavity to reach a point of high gain and then swiftly stopping the light transmission, the SA regulates the laser output in passive Q-switching. The production of high-energy pulses with a high peak power is the consequence of this technique. The repetition rate increases from 33.46 kHz at 83.6 mW to 77.96 kHz at 171.7 mW as the input power of the laser increases. The repetition rate drops somewhat from 52.96 kHz at 105.2 mW to 33.99 kHz at 116.3 mW.

Table 1
Q-Switched pulsed wave laser specifications

Q-Switched laser parameters	Value
Threshold LD pump - continuous wave	36.7 mW
Threshold LD pump - pulsed wave	48.2 mW
Highest LD pump - Pulsed wave	171.7 mW
Triggering repetition rate	33.46 kHz
Highest repetition rate	77.96 kHz
Triggering pulse width	11.36 µs
Lowest pulse width	4.033 µs
Highest output pulse energy	28.2 nJ
Highest output power	2.20 mW

Factors including the initial population inversion, the relaxation period, and the dynamics of energy transfer in the laser cavity can all have an impact on the relationship between input power and repetition rate in a passive Q-switched laser. These elements can change, based on any particular configuration and settings of the laser system.

The length of each laser pulse that the system emits is referred to as the pulse width. The SA effectively absorbs the incoming light when the laser input power is low, preventing it from passing into the laser cavity. As a result, until a specific threshold is achieved, the energy stored in the laser medium continues to increase.

The SA rapidly saturates once the threshold is reached, enabling the stored energy to be released in a brief, powerful pulse. Due to this technique, shorter-duration, high-energy laser pulses with a narrower pulse width are produced.

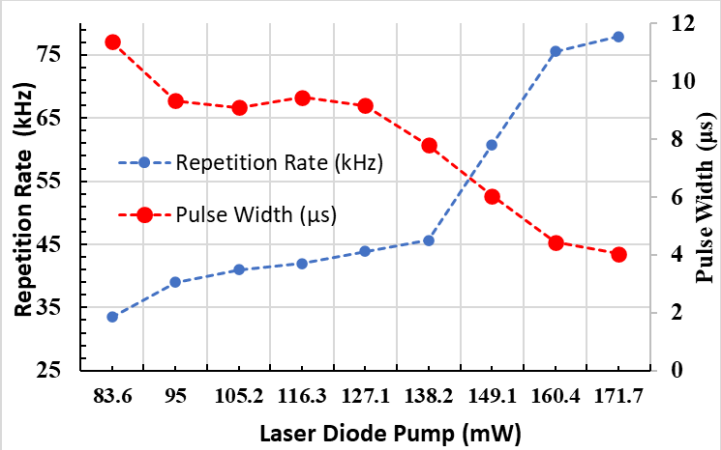

Fig. 7. Repetition rate of Q-switch with the LD pump

The pulse width typically tends to shrink with an increased repetition rate while retaining the same average power as the laser input power rises. From 11.36 µs at 83.6 mW to 4.033 µs at 171.7 mW, the pulse width drops. The SA saturates more quickly as the laser input power rises, allowing the energy to be released in a shorter duration producing a narrower pulse. It is vital to understand that the relationship is not purely linear. The pulse width does not necessarily become smaller as the laser input power rises.

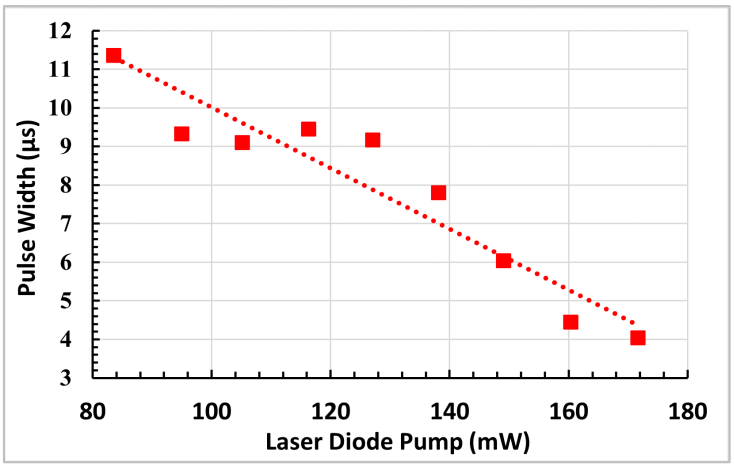

Fig. 8. Pulse width of Q-switch with the LD pump

The oscilloscope trace for each reading indicated that as the pump power was increased, the pulse repetition rate noticeably increased where the pulse width was reduced, as would be expected from a Q-switched cavity. Even at the maximum incident pump power of 171.7 mW, the Ag-SA material remains optically unaffected. Although the pulse width drops below 4 µs as pump power increases, it stabilises beyond 160 mW, at which time mode-locked systems might achieve pulse widths as low as in the nanoseconds range at a repetition rate in the kilohertz range.

The amount of energy that is included in each laser pulse that the cavity emits is referred to as the pulse energy. The SA rapidly saturates when the laser input power exceeds a particular level, allowing the energy to be released in a brief, strong pulse. High-energy laser pulses are produced by this method. The rising pulse energy readings from 1.413 nJ at 83.6 mW to 4.06 nJ at 116.3 mW show that the pulse energy typically tends to rise as the laser input power increases.

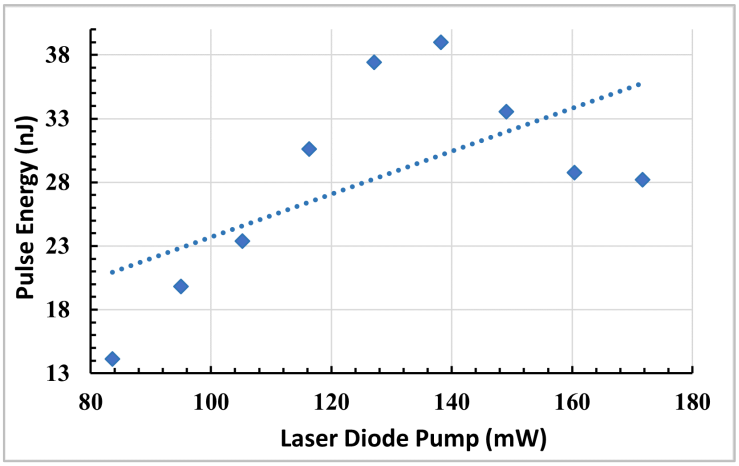

Fig. 9. Pulse width of Q-switch with the LD pump

Laser input power and pulse energy normally have a linear relationship. It is essentially noteworthy that the relationship may not always be precisely linear. Pulse energy can also be affected by other elements, including the initial population inversion, energy losses within the laser cavity, and the effectiveness of the energy extraction procedure. Comparative performance analysis of PQS fibre lasers employing Sn-SA is given in Table 2, where it was managed to achieve a 77.96 kHz repetition rate without bleaching of the SA at a pump power of 171.7 mW

Table 2
Performance of PQS fibre lasers employing Sn-SA

Spectrum (μm)	Max. stable pump(mW)	Max. pulse energy (nJ)	Min. pulse width (μs)	Rep. rate (Min) kHz	Rep. rate (max) kHz	SNR (dB)	Ref.
1500.0	135	57.8	2.3	-	62.4	45	[35]
1565.0	236.2	34.7	8.16	42.5	55.7	63	[23]
1564.5	139	132	2.4	17.9	58.5	-	[24]
1558.7	-	-	3.2	9.5	74.1	35	[36]
1500.0	228.8	67.3	4.2	38.3	56.2	57	[37]
1916.5	-	69.3	5.1	-	50.1	34.2	[38]
1535.0	37.8	27.5	11.85	15.1	28.4	-	[39]
1590.7	171.7	24.8	4.03	33.46	77.96	41	This work

4. Conclusions

This study has intrinsically evaluated the Ag-SA's effects on the passive Q-switched all-fibre laser's characteristics, including average output power, pulse energy, pulse width, and repetition rate. In an EDFL ring cavity design, the produced Ag-SA efficiently served as a Q-switcher. This passively Q-switched EDFL based on Ag achieves Q-switching at a wavelength of 1590.7 nm. The highest pulse repetition rate, the lowest pulse repetition interval, the minimum pulse width, and the duty cycle of the energetic Q-switching pulse have been found to be 77.96 kHz, 12.8μs, 4.03μs, and 0.334 respectively. Additionally, peak power and pulse energy have been determined to be 28.2 nJ and 2.21 mW respectively, with a maximum output power of 3.2 mW. The results of the investigation successfully established that the designed Ag-SA can function as a Q-switcher to produce a reliable and potent Q-switching pulse train within the 1.5-m spectral region.

Acknowledgement
The authors gratefully acknowledge the financial support of the Ministry of Higher Education Malaysia for their encouragement and grant support under the Fundamental Research Grant Scheme (FRGS/1/2020/TK0/UTM/02/46).

References

[1] Schulze, Sven, Michel Wehrhold, and Carsten Hille. "Femtosecond-pulsed laser written and etched fiber Bragg gratings for fiber-optical biosensing." *Sensors* 18, no. 9 (2018): 2844. https://doi.org/10.3390/s18092844
[2] Coradin, F. K., G. R. C. Possetti, R. C. Kamikawachi, M. Muller, and J. L. Fabris. "Etched fiber Bragg grating sensing system thermically assisted for analysis of water-ethanol mixtures." In *21st International Conference on Optical Fiber Sensors*, vol. 7753, pp. 1171-1174. SPIE, 2011. https://doi.org/10.1117/12.885088
[3] Gattass, Rafael R., and Eric Mazur. "Femtosecond laser micromachining in transparent materials." *Nature photonics* 2, no. 4 (2008): 219-225. https://doi.org/10.1038/nphoton.2008.47
[4] Eatemadi, Ali, Hadis Daraee, Hamzeh Karimkhanloo, Mohammad Kouhi, Nosratollah Zarghami, Abolfazl Akbarzadeh, Mozhgan Abasi, Younes Hanifehpour, and Sang Woo Joo. "Carbon nanotubes: properties, synthesis, purification, and medical applications." *Nanoscale research letters* 9 (2014): 1-13. https://doi.org/10.1186/1556-276X-9-393
[5] Sun, Guoqing, Ming Feng, Kang Zhang, Tianhao Wang, Yuanhao Li, Dongdong Han, Yigang Li, and Feng Song. "Q-Switched and Mode-Locked Er-doped fiber laser based on MAX phase Ti2AlC saturable absorber." *Results in Physics* 26 (2021): 104451. https://doi.org/10.1016/j.rinp.2021.104451
[6] Soong, H. Kaz, and João Baptista Malta. "Femtosecond lasers in ophthalmology." *American journal of ophthalmology* 147, no. 2 (2009): 189-197. https://doi.org/10.1016/j.ajo.2008.08.026
[7] Diddams, Scott A., Leo Hollberg, and Vela Mbele. "Molecular fingerprinting with the resolved modes of a femtosecond laser frequency comb." *Nature* 445, no. 7128 (2007): 627-630. https://doi.org/10.1038/nature05524
[8] Jhon, Young In, Jinho Lee, Young Min Jhon, and Ju Han Lee. "Ultrafast mode-locking in highly stacked Ti3C2Tx MXenes for 1.9-μm infrared femtosecond pulsed lasers." *Nanophotonics* 10, no. 6 (2021): 1741-1751. https://doi.org/10.1515/nanoph-2020-0678
[9] Sakr, Hesham, Yong Chen, Gregory T. Jasion, Thomas D. Bradley, John R. Hayes, Hans Christian H. Mulvad, Ian A. Davidson, Eric Numkam Fokoua, and Francesco Poletti. "Hollow core optical fibres with comparable attenuation to silica fibres between 600 and 1100 nm." *Nature communications* 11, no. 1 (2020): 6030. https://doi.org/10.1038/s41467-020-19910-7
[10] Lee, Jinho, Suhyoung Kwon, and Ju Han Lee. "Ti 2 AlC-based saturable absorber for passive Q-switching of a fiber laser." *Optical materials express* 9, no. 5 (2019): 2057-2066. https://doi.org/10.1364/OME.9.002057
[11] Kratky, Alexander, Dieter Schuöcker, and Gerhard Liedl. "Processing with kW fibre lasers: advantages and limits." In *XVII International Symposium on Gas Flow, Chemical Lasers, and High-Power Lasers*, vol. 7131, pp. 493-504. SPIE, 2009. https://doi.org/10.1117/12.816655
[12] Andrés, M. V., J. L. Cruz, A. Díez, P. Pérez-Millán, and M. Delgado-Pinar. "Actively Q-switched all-fiber lasers." *Laser Physics Letters* 5, no. 2 (2008): 93-99. https://doi.org/10.1002/lapl.200710104
[13] Ahmad, H., N. N. Ismail, S. N. Aidit, S. A. Reduan, M. Z. Samion, and N. Yusoff. "2.08 μm Q-switched holmium fiber laser using niobium carbide-polyvinyl alcohol (Nb2C-PVA) as a saturable absorber." *Optics Communications* 490 (2021): 126888. https://doi.org/10.1016/j.optcom.2021.126888
[14] Kaur, Mandeep, Geoffrey Hohert, Pierre M. Lane, and Carlo Menon. "Fabrication of a stepped optical fiber tip for miniaturized scanners." *Optical Fiber Technology* 61 (2021): 102436. https://doi.org/10.1016/j.yofte.2020.102436
[15] You, J. W., S. R. Bongu, Q. Bao, and N. C. Panoiu. "Nonlinear optical properties and applications of 2D materials: theoretical and experimental aspects." *Nanophotonics* 8, no. 1 (2018): 63-97. https://doi.org/10.1515/nanoph-2018-0106
[16] Martinez, Amos, Mohammed Al Araimi, Artemiy Dmitriev, Petro Lutsyk, Shen Li, Chengbo Mou, Alexey Rozhin, Misha Sumetsky, and Sergei Turitsyn. "Low-loss saturable absorbers based on tapered fibers embedded in carbon nanotube/polymer composites." *APL Photonics* 2, no. 12 (2017). https://doi.org/10.1063/1.4996918
[17] Boetti, Nadia Giovanna, Diego Pugliese, Edoardo Ceci-Ginistrelli, Joris Lousteau, Davide Janner, and Daniel Milanese. "Highly doped phosphate glass fibers for compact lasers and amplifiers: a review." *Applied Sciences* 7, no. 12 (2017): 1295. https://doi.org/10.3390/app7121295
[18] Liu, Xing, Qun Gao, Yang Zheng, Dong Mao, and Jianlin Zhao. "Recent progress of pulsed fiber lasers based on transition-metal dichalcogenides and black phosphorus saturable absorbers." *Nanophotonics* 9, no. 8 (2020): 2215-2231. https://doi.org/10.1515/nanoph-2019-0566

[19] Keller, Ursula, Kurt J. Weingarten, Franz X. Kartner, Daniel Kopf, Bernd Braun, Isabella D. Jung, Regula Fluck, Clemens Honninger, Nicolai Matuschek, and J. Aus Der Au. "Semiconductor saturable absorber mirrors (SESAM's) for femtosecond to nanosecond pulse generation in solid-state lasers." *IEEE Journal of selected topics in QUANTUM ELECTRONICS* 2, no. 3 (1996): 435-453. https://doi.org/10.1109/2944.571743

[20] Yang, Zixin, Lili Han, Jiabao Zhang, Yupeng Zhang, Feng Zhang, Zhitao Lin, Xianghe Ren, Qi Yang, and Han Zhang. "Passively Q-switched laser using PtSe2 as saturable absorber at 1.3 μm." *Infrared Physics & Technology* 104 (2020): 103155. https://doi.org/10.1016/j.infrared.2019.103155

[21] Muhammad, Ahmad Razif, Rozalina Zakaria, Muhammad Taufiq Ahmad, Pengfei Wang, and Sulaiman Wadi Harun. "Pure gold saturable absorber for generating Q-switching pulses at 2 μm in thulium-doped fiber laser cavity." *Optical Fiber Technology* 50 (2019): 23-30. https://doi.org/10.1016/j.yofte.2019.02.010

[22] Glubokov, Dmitrii Anatol'evich, Vladimir Vasil'evich Sychev, Aleksandr Sergeevich Mikhailov, Andrei Evgen'evich Korolkov, Dmitrii Anatol'evich Chubich, Boris Isaakovich Shapiro, and Alexey Grigor'evich Vitukhnovskii. "Saturable absorber based on silver nanoparticles for passively mode-locked lasers." *Quantum Electronics* 44, no. 4 (2014): 314. https://doi.org/10.1070/QE2014v044n04ABEH015353

[23] Rosdin, R. Z. R., M. T. Ahmad, Z. Jusoh, H. Arof, and S. W. Harun. "All-fiber Q-switched fiber laser based on silver nanoparticles saturable absorber." *Digest Journal of Nanomaterials and Biostructures* 13 (2018): 1159-1164.

[24] Guo, Hao, Ming Feng, Feng Song, Haoyu Li, Aibing Ren, Xukang Wei, Yigang Li, Xiaoxuan Xu, and Jianguo Tian. "$ Q $-Switched Erbium-Doped Fiber Laser Based on Silver Nanoparticles as a Saturable Absorber." *IEEE Photonics Technology Letters* 28, no. 2 (2015): 135-138. https://doi.org/10.1109/LPT.2015.2487521

[25] Liu, Xing, Qun Gao, Yang Zheng, Dong Mao, and Jianlin Zhao. "Recent progress of pulsed fiber lasers based on transition-metal dichalcogenides and black phosphorus saturable absorbers." *Nanophotonics* 9, no. 8 (2020): 2215-2231. https://doi.org/10.1515/nanoph-2019-0566

[26] Hashmi, M. Saleem J. *Comprehensive materials processing*. Newnes, 2014.

[27] Eatemadi, Ali, Hadis Daraee, Hamzeh Karimkhanloo, Mohammad Kouhi, Nosratollah Zarghami, Abolfazl Akbarzadeh, Mozhgan Abasi, Younes Hanifehpour, and Sang Woo Joo. "Carbon nanotubes: properties, synthesis, purification, and medical applications." *Nanoscale research letters* 9 (2014): 1-13. https://doi.org/10.1186/1556-276X-9-393

[28] Rudko, G. Yu, A. O. Kovalchuk, V. I. Fediv, Q. Ren, W. M. Chen, I. A. Buyanova, and Galia Pozina. "Role of the host polymer matrix in light emission processes in nano-CdS/poly vinyl alcohol composite." *Thin Solid Films* 543 (2013): 11-15. https://doi.org/10.1016/j.tsf.2013.04.035

[29] Ahmad, Harith, Rosli Ramli, Norhasliza Yusoff, Muhamad Zharif Samion, M. F. Ismail, L. Bayang, Siti Nabila Aidit, A. K. Zamzuri, and K. Thambiratnam. "155 nm-wideband and tunable q-switched fiber laser using an MXene Ti3C2TX coated microfiber based saturable absorber." *Laser Physics Letters* 17, no. 8 (2020): 085103. https://doi.org/10.1088/1612-202X/aba0bd

[30] Musthafa, Kawther M., Azura Hamzah, Ooi Wei Ling, Ahmad Haziq Aiman Rosol, Norliza Mohamed, Mahroof Mohamed Mafroos, and Sulaiman Wadi Harun. "Synthesisation, Fabrication, and Incorporation Techniques of MAX Phase and MXene Saturable Absorber in Passively Q-switched and Mode-locked All-fibre Laser Cavities: A Review." *Journal of Advanced Research in Applied Sciences and Engineering Technology* 32, no. 2 (2023): 119-141. https://doi.org/10.37934/araset.32.2.119141

[31] Lokman, Muhammad Quisar, Muhammad Farid Mohd Rusdi, Ahmad Haziq Aiman Rosol, Fauzan Ahmad, Suhaidi Shafie, Hafizal Yahaya, Rizuan Mohd Rosnan, Mohd Azizi Abdul Rahman, and Sulaiman Wadi Harun. "Synthesis of silver nanoparticles using chemical reduction techniques for Q-switcher at 1.5 μm region." *Optik* 244 (2021): 167621. https://doi.org/10.1016/j.ijleo.2021.167621

[32] Lokman, Muhammad Quisar, Suhaidi Shafie, Suraya Shaban, Fauzan Ahmad, Haslina Jaafar, Rizuan Mohd Rosnan, Hafizal Yahaya, and Shahrum Shah Abdullah. "Enhancing photocurrent performance based on photoanode thickness and surface plasmon resonance using Ag-TiO2 nanocomposites in dye-sensitized solar cells." *Materials* 12, no. 13 (2019): 2111. https://doi.org/10.3390/ma12132111

[33] Mehta, B. K., Meenal Chhajlani, and B. D. Shrivastava. "Green synthesis of silver nanoparticles and their characterization by XRD." In *Journal of physics: conference series*, vol. 836, no. 1, p. 012050. IOP Publishing, 2017. https://doi.org/10.1088/1742-6596/836/1/012050

[34] Pillai, Zeena S., and Prashant V. Kamat. "What factors control the size and shape of silver nanoparticles in the citrate ion reduction method?." *The Journal of Physical Chemistry B* 108, no. 3 (2004): 945-951. https://doi.org/10.1021/jp037018r

[35] Lyu, Wenhao, Yuan Cheng, Jiayi An, Marcello Condorelli, Mario Pulvirenti, Giuseppe Compagnini, Xiaogang Wang, Bo Fu, and Vittorio Scardaci. "Silver Nanoplate Composites as Nonlinear Saturable Absorbers for a Q-Switched Laser." In *Photonics*, vol. 9, no. 11, p. 835. MDPI, 2022. https://doi.org/10.3390/photonics9110835

[36] Ahmad, Harith, N. E. Ruslan, Mohd Afiq Ismail, Z. A. Ali, S. A. Reduan, C. S. J. Lee, and Sulaiman Wadi Harun. "Silver nanoparticle-film based saturable absorber for passively Q-switched erbium-doped fiber laser (EDFL) in ring cavity configuration." *Laser Physics* 26, no. 9 (2016): 095103. https://doi.org/10.1088/1054-660X/26/9/095103

[37] Ahmad, Harith, M. Z. Samion, A. Muhamad, A. S. Sharbirin, and Mohammad Faizal Ismail. "Passively Q-switched thulium-doped fiber laser with silver-nanoparticle film as the saturable absorber for operation at 2.0 µm." *Laser Physics Letters* 13, no. 12 (2016): 126201. https://doi.org/10.1088/1612-2011/13/12/126201

[38] Ahmad, H., M. Z. Samion, A. Muhamad, A. S. Sharbirin, R. A. Shaharuddin, K. Thambiratnam, S. F. Norizan, and M. F. Ismail. "Tunable 2.0 µm Q-switched fiber laser using a silver nanoparticle based saturable absorber." *Laser Physics* 27, no. 6 (2017): 065110. https://doi.org/10.1088/1555-6611/aa6da0

[39] Rizman, Zairi Ismael, Muhammad Farid Mohd Rusdi, Moh Yasin, P. Yupapin, and Sulaiman Wadi Harun. "Q-switched tunable fiber laser utilizing silver nanoparticles deposited onto PVA film as saturable absorber." *Indian Journal of Physics* 95 (2021): 141-145. https://doi.org/10.1007/s12648-019-01675-5